DEVELOPMENT OF A TABULAR MANOEUVRING MODEL FOR HULL FORCES APPLIED TO FULL AND SLENDER SHIPS IN SHALLOW WATER

Katrien Eloot (Flanders Hydraulics Research, Belgium)
Marc Vantorre (Ghent University, Belgium)

Abstract: Most formulations of mathematical modelling of ship manoeuvres in shallow water discussed in literature are based on expressions for the deep water case. Several usual and unusual phenomena occurring during manoeuvres at limited under keel clearance (10% to 50%) are not considered. A tabular model for the hull forces is proposed, taking the shallow water condition as starting point, with the intention to cover wide ranges of kinematical parameters so that a great variety of manoeuvres can be simulated. The implementation of the mathematical model is based on captive model tests with 4 m models of the tanker *Esso Osaka* and a fourth generation container carrier. The experimental program consists of well-known, classical PMM test types combined with alternative tests. Preliminary guidelines are formulated for the selection of test parameters, taking account of their influence on the hydrodynamic coefficients.

1. INTRODUCTION

The development of a mathematical model describing ship manoeuvres in varying conditions holds on many researchers since decades. Although some of them ask themselves whether "one can have a general, standardised manoeuvring model" [1], at this moment standardisation is still far away.

The mathematical models published in literature can be divided into two groups: models based on a pure analytical approach (*pure regression models*) and models taking account of the underlying physical phenomena (*modular simulation models*). The latter provides many possibilities as the manoeuvring vessel is considered as a composition of interacting parts, hull, propeller and rudder, each represented by a separate module. On the other hand, the determination of the hydrodynamic forces acting on each part and, particularly, the interaction terms can become complex in case of manoeuvres in navigation areas characterised by limitations in both width and depth, such as harbours and approach channels.

Although numerical methods based on CFD (Computational Fluid Dynamics) are becoming more and more popular to be used for the determination of hydrodynamic forces, the efforts have still not made model testing unnecessary, especially in shallow water. Calculations in very shallow water ($h/T<1.2$) and even shallow water ($h/T<1.5$) are scarce and the quantitative agreement in these conditions is rather poor [2].

The paper intends:

- to give a description of the general structure of a tabular model for the hydrodynamic forces acting on a ship's hull during manoeuvres in shallow, unrestricted water;
- to implement this mathematical model for the well-known VLCC *Esso Osaka* and a container carrier based on results of captive model tests;
- to suggest some guidelines for a standardised physical test program in shallow water conditions.

2. MATHEMATICAL MODEL: GENERAL STRUCTURE

2.1 Conditions

The tabular model for hull forces in shallow and unrestricted water has to fulfil the following conditions:

- limited under keel clearances;
- speed limitations;
- four quadrants of operation during harbour manoeuvres such as drifting and swinging;
- due to the low ship velocities the ship motions become time dependent and memory effects may occur.

The model only describes the hydrodynamic forces acting on the ship hull during a combination of surge-sway-yaw motions. Roll motion is neglected due to the low ship velocities.

2.2 Hull forces and moment

The equations of motion of a manoeuvring ship are:

$$\begin{aligned} m\left(\dot{u} - vr - x_G r^2\right) &= X_H + X_P + X_R \\ m\left(\dot{v} + ur + x_G \dot{r}\right) &= Y_H + Y_P + Y_R \\ I_{zz}\dot{r} + mx_G\left(\dot{v} + ur\right) &= N_H + N_P + N_R \end{aligned} \quad (1)$$

with $_H$ hull, $_P$ propeller and $_R$ rudder.

Hull force components are mainly caused by accelerations and velocities.

$$\begin{aligned} X_H &= X_{\dot{u}}\dot{u} + X^{(\beta)}(u,v,0) + X^{(\gamma)}(u,0,r) + X^{(\beta,\gamma)}(0,v,r) \\ Y_H &= Y_{\dot{v}}\dot{v} + Y_{\dot{r}}\dot{r} + Y^{(\beta)}(u,v,0) + Y^{(\gamma)}(u,0,r) \\ &\quad + Y^{(\beta,\gamma)}(0,v,r) \\ N_H &= N_{\dot{r}}\dot{r} + N_{\dot{v}}\dot{v} + N^{(\beta)}(u,v,0) + N^{(\gamma)}(u,0,r) \\ &\quad + N^{(\beta,\gamma)}(0,v,r) \end{aligned} \quad (2)$$

The velocity dependent forces in (2) are expressed as tabular models, the following angles varying over four quadrants from -180° to 180°:

$$\beta = \text{Arc}\tan\left(\frac{-v}{u}\right) \quad (3)$$

$$\gamma = \text{Arc}\tan\left(\frac{rl}{u}\right) = \text{Arc}\tan\left(\frac{rL_{pp}}{2u}\right) \quad (4)$$

$$\text{Arc}\tan\left(\frac{rl}{v}\right) = \text{Arc}\tan\left(\frac{rL_{pp}}{2v}\right) \quad (5)$$

The expressions $f^{(\beta)}(u,v,0)$, $f^{(\gamma)}(u,0,r)$ and $f^{(\beta,\gamma)}(0,v,r)$ with f = X, Y or N are, respectively, the forces or moment measured during pure sway, pure yaw or the additional forces measured during a combination of sway and yaw. β is the drift angle, γ is the yaw rate angle and the angle indicated by $\text{Arc}\tan(rl/v)$ has no specific name as it is based on the ratio of yaw rate to side velocity which are already used in the expressions (3) and (4) [3].

Non-dimensional expressions for the velocity dependent forces and yawing moment are formulated as follows:

- pure sway:

$$X', Y' = \frac{X, Y}{0.5\rho L_{PP} d\left(u^2 + v^2\right)} \quad (6)$$

$$N' = \frac{N}{0.5\rho L_{PP}^2 d\left(u^2 + v^2\right)} \quad (7)$$

- pure yaw:

$$X', Y' = \frac{X, Y}{0.5\rho L_{PP} d\left(u^2 + (rl)^2\right)} \quad (8)$$

$$N' = \frac{N}{0.5\rho L_{PP}^2 d\left(u^2 + (rl)^2\right)} \quad (9)$$

- combination sway-yaw:

$$X', Y' = \frac{X, Y}{0.5\rho L_{PP} d\left(v^2 + (rl)^2\right)} \quad (10)$$

$$N' = \frac{N}{0.5\rho L_{PP}^2 d\left(v^2 + (rl)^2\right)} \quad (11)$$

Acceleration dependent coefficients are made non-dimensional based on the length between perpendiculars and the draught.

$$X'_{\dot{u}}, Y'_{\dot{v}} = \frac{X_{\dot{u}}, Y_{\dot{v}}}{0.5\rho L_{PP}^2 d} \quad (12)$$

$$Y'_{\dot{r}}, N'_{\dot{v}} = \frac{Y_{\dot{r}}, N_{\dot{v}}}{0.5\rho L_{PP}^3 d} \quad (13)$$

$$N'_{\dot{r}} = \frac{N_{\dot{r}}}{0.5\rho L_{PP}^4 d} \quad (14)$$

3. CAPTIVE MODEL TEST PROGRAM

3.1 Ship models and test conditions

In accordance to the full scale trials reported by Crane [4], the shallow water conditions during the captive tests with the Esso Osaka model correspond to under keel clearances of 20% and 50%. No model tests were carried out in deep water. The container carrier D is tested at under keel clearance values of 20% and 7% of the ship's draught. The captive model tests were executed with a fully automated PMM-carriage at the *Towing Tank for Manoeuvres in Shallow Water* (*co-operation Flanders Hydraulics Research – Ghent University*), Antwerp (Belgium). The main characteristics of the towing tank are 88 x 7 x 0.5 m³, with a useful length of 68 m.

Hull characteristics are summarised in table 1 and body plans are shown in figure 1.

Table 1 Geometrical characteristics

Esso Osaka E		Container carrier D	
L_{OA}	343.0 m	L_{OA}	301.5 m
L_{PP}	325.0 m	L_{PP}	289.8 m
B	53.0 m	B	40.3 m
d	21.8 m	d	15.0 m
C_B	0.83	C_B	0.61
scale	1:85	Scale	1:75

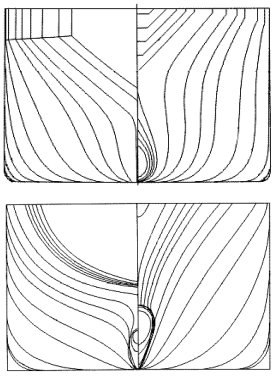

Fig. 1. Body plans of tanker Esso Osaka and container carrier D.

The draught of the container carrier is slightly higher than the maximum draught of the largest existing containerships (d = 14.5 m).

3.2. Test program

The test program consisted of following test types:

Stationary model tests:
- straight-line tests with positive and negative forward speed;
- oblique towing tests with positive and negative forward speed.

Non-stationary model tests:
- oscillatory tests in x- and y-direction and around ψ-axis;
- harmonic sway tests: pure sway;
- alternative sway tests: pure sway;
- harmonic yaw tests: pure yaw, yaw with drift with positive and negative forward speed;
- multimodal tests.

No circular motion tests have been executed due to a lack of a rotating arm facility. Thanks to the execution of harmonic tests with varying test frequency, motion amplitude and carriage speed, a wide range of yaw rate angles was covered.

4. ACCELERATION DEPENDENT COEFFICIENTS

4.1 Surge motion

Figure 2 shows the ratio of the added mass for surge ($m_x = -X_{\dot{u}}$) to the ship's mass m, based on oscillatory tests. The influence of test frequency or amplitude appears to be small.

4.2 Sway motion

According to the sensitivity analysis in [5], the added mass due to sway $Y_{\dot{v}}$ is a very important parameter for the prediction of ship manoeuvrability.

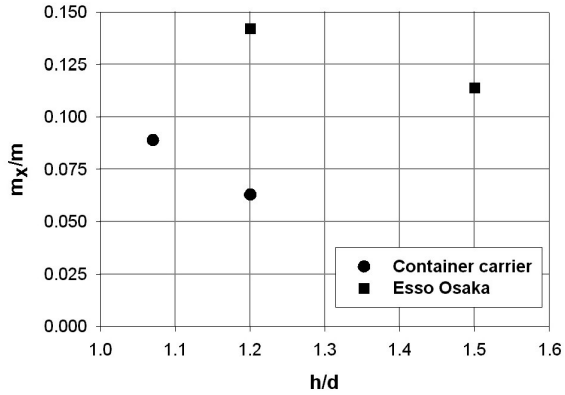

Fig. 2. Ratio of the surge added mass m_x to the ship's mass m as function of depth to draught ratio.

Classical PMM sway tests and alternative sway tests have been executed with varying model speed, test frequency and sway amplitude. In shallow water conditions the influence of these test parameters cannot be neglected. Although a non-conventional sway test was introduced in [6], non-stationary effects could not be eliminated.

The added mass for sway shown in figures 3 and 4 is based on classical sway tests (F_n = 0.032 and 0.065) and oscillatory tests at zero speed. During the latter, the non-dimensional test frequency $\omega' = \omega L_{PP}/u$ reaches infinity so that the added mass at infinite frequency is displayed after the axis breaks in figures 3 and 4.

The largest absolute value for the sway acceleration derivative is measured during oscillatory tests (infinite frequency). Due to the scatter at lower frequencies an extrapolation to a quasi-stationary zero frequency value for the derivative cannot be determined.

In [6] it was discussed in which way tests have to be executed in order to obtain accurate results for the

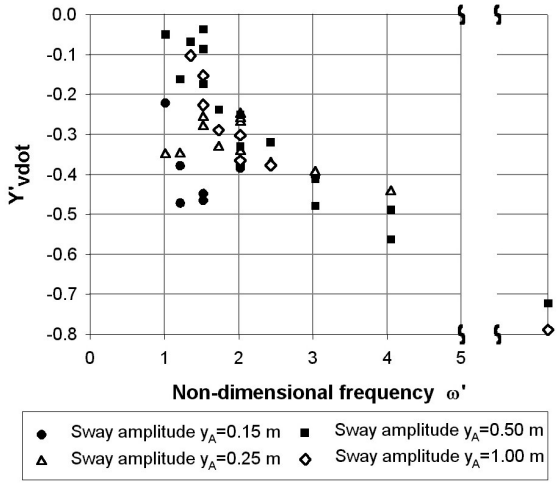

Fig. 3 Sway added mass Y'_{vdot} as function of non-dimensional frequency ω' during harmonic sway and oscillatory tests for D, 20% UKC.

acceleration derivative; it was concluded that a small sway amplitude and/or a high frequency are recommended.

In figure 4 the sway acceleration derivative is shown for the tanker and the container carrier based on sway tests with identical sway amplitudes of 0.5 m. As the under keel clearance decreases, the difference between acceleration derivatives measured at high and low frequencies becomes very important. For the container carrier at 7% UKC, even a sign change is observed as the frequency decreases.

In reply to the assumptions of other researchers reported in [6], the relationship between the acceleration derivative and the net under keel clearance during harmonic sway tests was studied.

During stationary straight ahead tests the net under keel clearance decreases approximately with the square of the ship's velocity or the Froude number (figure 5). At a full scale velocity of 12 knots the nominal UKC of 7% for the container carrier reduces to an UKC of 3% of the ship's draught.

During harmonic sway tests sway acceleration is in phase with the lateral position. As maximum sinkage

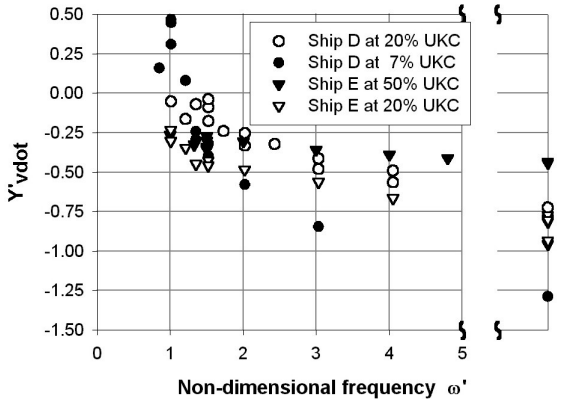

Fig. 4 Y'_{vdot} as function of non-dimensional frequency for harmonic sway and oscillatory tests with a sway amplitude of 0.5 m.

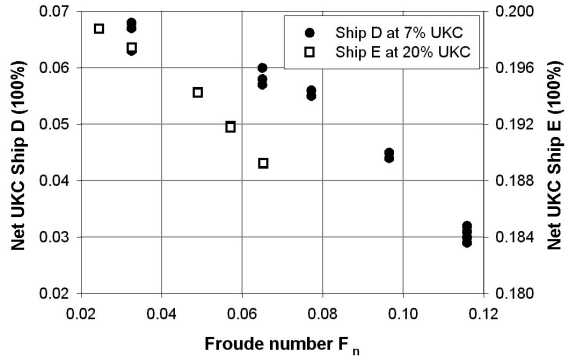

Fig. 5 Net UKC as function of Froude number during resistance tests without propeller action.

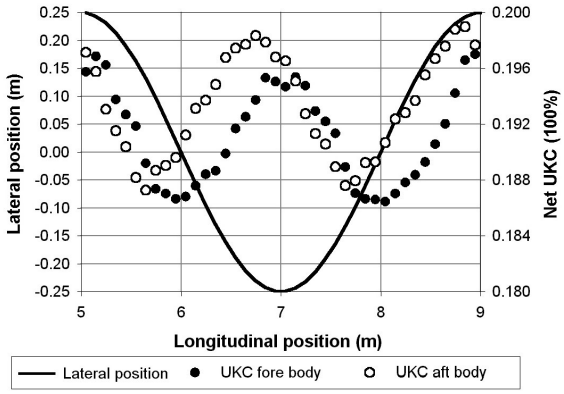

Fig. 6 Net UKC measured during a harmonic sway test (F_n = 0.033; ω' = 6; y_A = 0.25 m) for the Esso Osaka at a nominal UKC of 20%.

occurs near maximum sway velocity (figure 6) high added masses at high frequencies cannot be explained by squat effects.

The sway acceleration derivative of the yawing moment is less important. Mean values summarised in table 2 are based on the first period during alternative sway tests [6].

Table 2 Sway acceleration derivative N'_v

h/d	1.07	1.2
Container carrier D518	0.083	0.016
h/d	1.2	1.5
Tanker *Esso Osaka*	-0.016	-0.022

4.3 Yaw motion

Harmonic yaw tests have been executed with positive and negative speed. For full ships the added moment of inertia is rather insensitive to the selected test parameters during harmonic yaw tests. For slender ships the absolute value of the acceleration derivative increases slightly with increasing frequency during harmonic yaw and oscillatory tests. In figure 7 the added moment of inertia N'_f is displayed in function of the non-dimensional frequency ω' for harmonic yaw tests (F_n = 0.033) and oscillatory tests.

For the ship going astern, the added moment of inertia does not differ from the derivative for positive ship's speed both in magnitude and sign.

The selected value of the yaw amplitude has an important influence on the acceleration derivative of lateral force. According to [6] there are indications that conventional PMM yaw tests give more reliable results at high yaw amplitude. In addition, first order harmonic force components measured on fore (F) and aft body (A) proportional to the yaw acceleration (cosine) change in magnitude if the ship is going astern compared to going ahead. If a ship is going ahead, the lateral force proportional to the

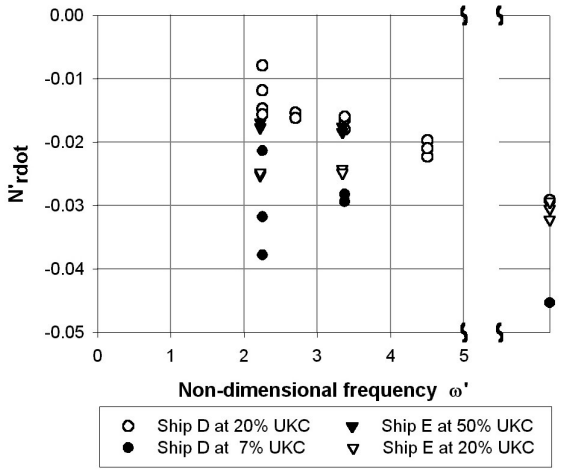

Fig. 7 Added moment of inertia for ship D and E.

acceleration is concentrated on the fore body during yaw motion (table 3). Going astern, maximum forces are measured on the aft body. This results in a change of sign for the yaw acceleration derivative of lateral force.

Table 3 First harmonic force components (tanker E)

			cosine (N)		sine (N)	
run	F_n	$\|\omega'\|$	(F)	(A)	(F)	(A)
EGGH08	0.016	3.34	-4.4	1.4	-4.3	3.9
EGGI02	-0.016	3.34	-1.7	3.7	-1.8	5.0

In [5] the derivative Y'_f is regarded as a parameter of small importance. Although the influence of test parameters is neglected in figure 8 by showing mean values during ahead motion, a sensitivity analysis must give a definitive answer about the importance of the acceleration derivative due to yaw and thus the test parameters on ship's manoeuvrability.

Compared to the results of pure yawing tests, the acceleration derivatives of the lateral force and yawing moment are affected by combining yaw and drift, depending on the hull form and the test parameters.

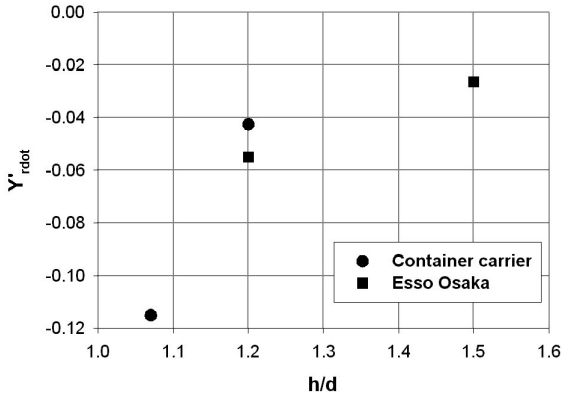

Fig. 8 Mean value of yaw acceleration derivative of lateral force Y'_{rdot} based on harmonic yaw tests.

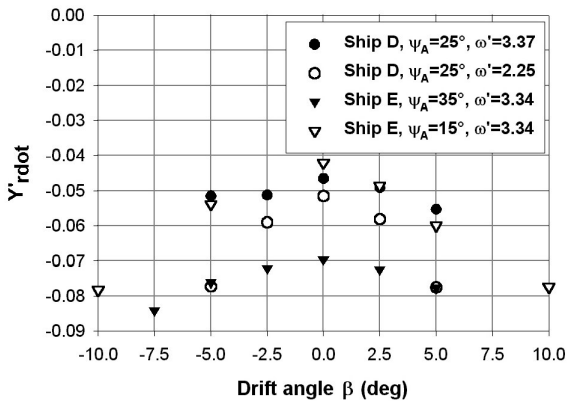

Fig. 9 Influence of drift angle on yaw acceleration derivative of lateral force Y'_{rdot} based on combined yawing and drifting tests.

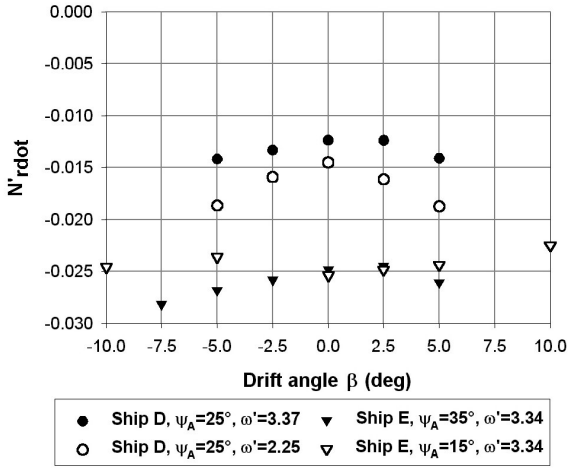

Fig. 10 Influence of drift angle on added moment of inertia N'_{rdot} based on combined yawing and drifting tests.

According to figure 9 and 10, the influence of a constant drift angle during a harmonic yawing test appears to be more significant for the acceleration derivative of lateral force both for slender and full ships and for the added moment of inertia of slender ships. The effect of drift is most important at low yaw amplitude ψ_A and/or low non-dimensional frequency ω'. Nevertheless, the increase of the derivatives is more or less symmetrical for positive and negative drift angles.

5. VELOCITY DEPENDENT TABULAR MODELS

5.1 Pure sway motion

The longitudinal force $X'^{(\beta)}$ measured during oblique towing is affected by the hull form and the water depth to draught ratio. For full ships the longitudinal hull force turns from a resistance force acting aft into a component acting forward as the drift angle increases (figure 11). The involved drift angle at

which this effect occurs, is getting smaller as the water depth decreases (see also [7]). For slender ships this force component keeps on acting aft ward during a large range of drift angles and only becomes positive when the ship is moving astern.

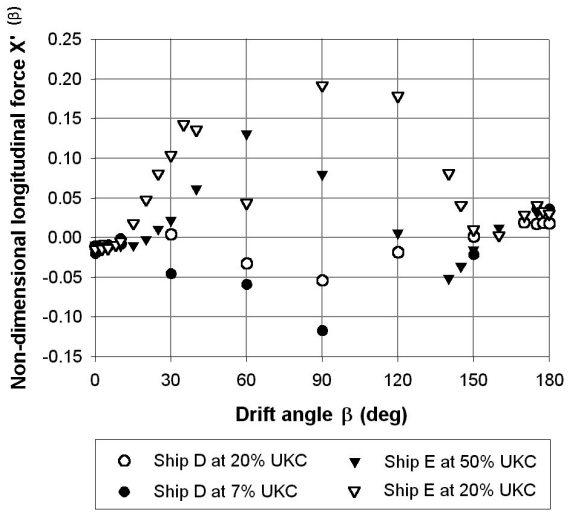

Fig. 11 Non-dimensional longitudinal force $X'^{(\beta)}$ modelled for full and slender ships based on oblique towing tests.

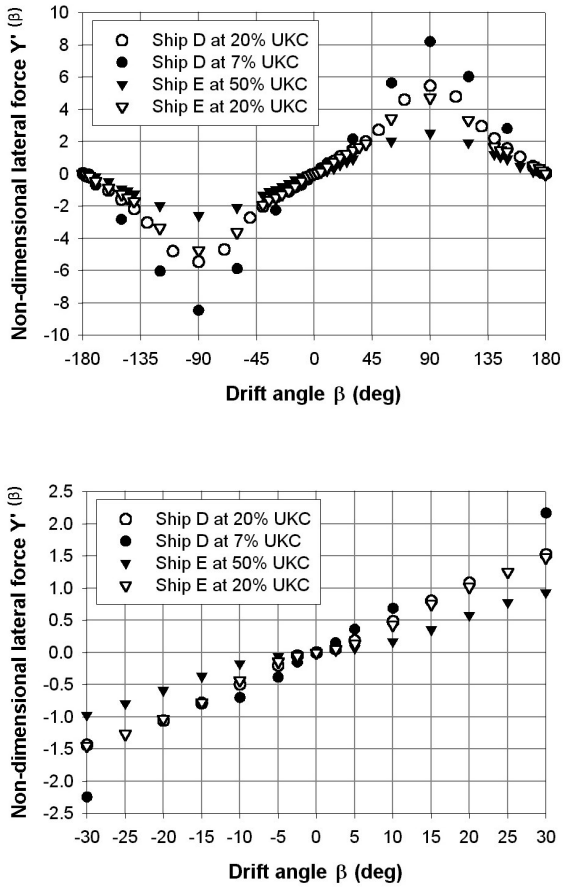

Fig. 12 Non-dimensional lateral force $Y'^{(\beta)}$ modelled for full and slender ships based on oblique towing tests.

The tabular models shown in figure 11 are based on hull forces measured during stationary and multi-modal oblique towing tests with propeller action [8].

Total lateral force and yawing moment measured during pure sway and pure yaw are caused by [3]:

- ideal fluid effects
- lifting effects
- cross flow effects.

As the under keel clearance decreases, cross flow induces important lateral forces around 90° drift angle (figure 12). A part of this force must be attributed to the presence of the rudder.

Due to a non-dimensional description of the lateral force based on the lateral underwater surface $L_{pp}d$, the tabular models for the tanker and the container carrier at 20% UKC differ hardly.

Nevertheless, for the ship moving astern the application point of this lateral force is situated more aft in the case of the tanker, compared to the container carrier (figure 13).

Additionally, the influence of a decreasing water depth on the yawing moment due to pure sway is more significant for the tanker than for the container carrier.

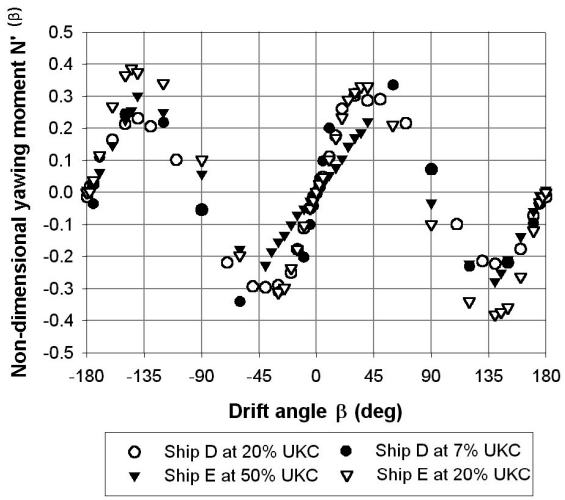

Fig. 13 Non-dimensional yawing moment $N'^{(\beta)}$ modelled for full and slender ships based on oblique towing tests.

5.2 Pure yaw motion

As no rotating arm facility is available, all results for pure yawing are based on harmonic PMM yaw tests.

Compared to the acceleration derivative of lateral force due to yawing, testing parameters frequency and yaw amplitude have a significant influence on the velocity dependent lateral force $Y'^{(\gamma)}$ both for full and slender ships.

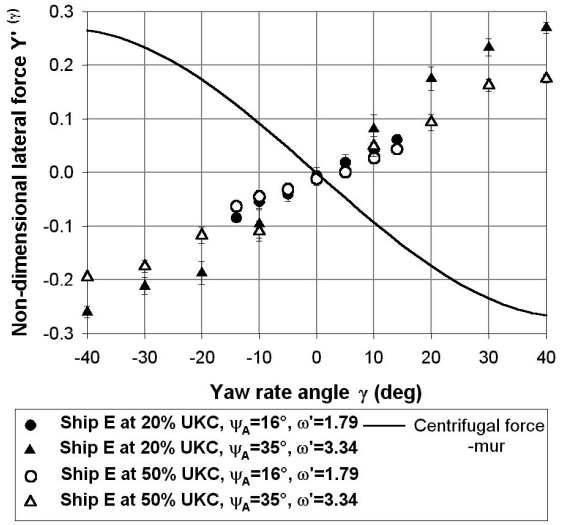

Fig. 14 Influence of frequency and yaw amplitude on non-dimensional lateral force $Y'^{(\gamma)}$ for the tanker.

In figure 14 the tabular models of individual test runs (F_n = 0.033) are compared for the tanker at the two available water depths. At 50% UKC the difference between the models based on runs at small frequency/small yaw amplitude or large frequency/large yaw amplitude is noticeable but small. At 20% UKC, on the other hand, the test parameters affect the resulting lateral force. The centrifugal force, -mur, proportional to the ship's mass m is added to the figures of $Y'^{(\gamma)}$.

The influence of the test parameters can partly be explained based on the sinkage measured during harmonic yaw tests. Maximum sinkage occurs at maximum yaw velocity or yaw rate angle and increases with decreasing water depth and increasing frequency and yaw amplitude (figure 15).

Moreover, the involved test parameters during pure yaw tests with slender ships influence both the magnitude and the sign of the lateral force $Y'^{(\gamma)}$ at small yaw rate angles.

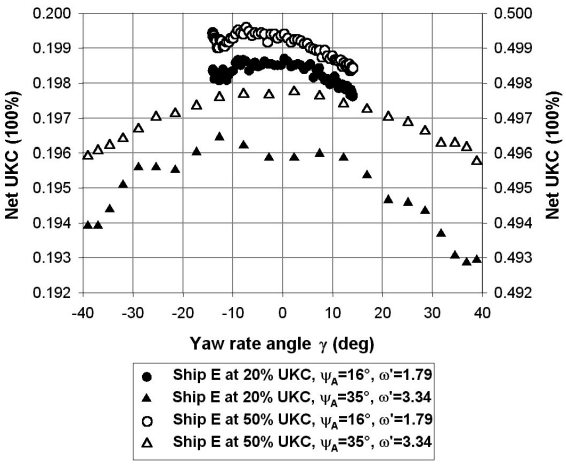

Fig. 15 Net UKC during harmonic yaw tests at under keel clearances of 20 and 50%.

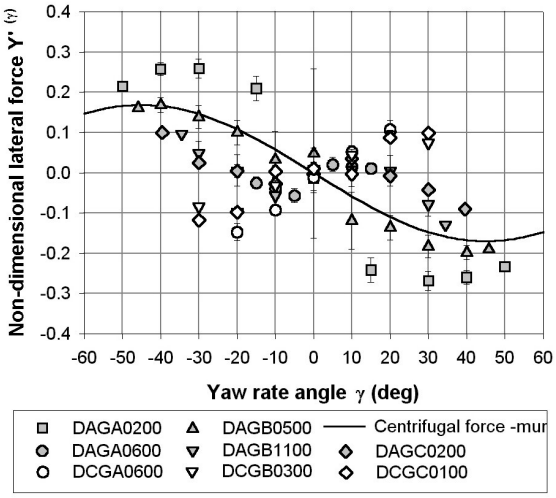

Fig. 16 Influence of frequency and yaw amplitude on non-dimensional lateral force $Y'^{(\gamma)}$ for the container carrier (see table 4 for test parameters).

Table 4 Test parameters for container carrier

Run	UKC	F_n	ψ_A	ω'
DAGA02	20%	0.033	35°	4.5
DAGA06	20%	0.033	15°	2.3
DAGB05	20%	0.049	35°	3.4
DAGB11	20%	0.049	35°	2.3
DAGC02	20%	0.065	35°	2.7
DCGA06	7%	0.033	15°	2.3
DCGB03	7%	0.049	30°	2.3
DCGC01	7%	0.065	25°	2.7

With increasing frequency (ω' > 3) the centrifugal force increases with the hydrodynamic lateral force $Y'^{(\gamma)}$ even at yaw rate angles around zero degrees. As the water depth to draught ratio decreases to very shallow water (UKC of 7%), hydrodynamic force $Y'^{(\gamma)}$ is opposite to the centrifugal force line so that hydrodynamic force and centrifugal force neutralise each other.

Contrary to the lateral force, the yawing moment is scarcely influenced by the test parameters during pure yaw tests. Tabular models during individual test runs (F_n = 0.033; ω' = 3.8; ψ_A = 35°) for the tanker and the container carrier are shown in figure 17. Similar to the lateral force due to pure swaying, the difference between non-dimensional yawing moment $N'^{(\gamma)}$ at 20% UKC for slender and full ships is small.

Four quadrants tabular models for the tanker at an UKC of 20% of the ship's draught are illustrated in figure 18. Values at 90° yaw rate angle are based on oscillating tests around ψ-axis (zero forward velocity) which are affected by memory effects caused by the ship going through his own wake. Therefore, 90° values were calculated based on the first cycle of oscillating tests during which memory effects are restricted.

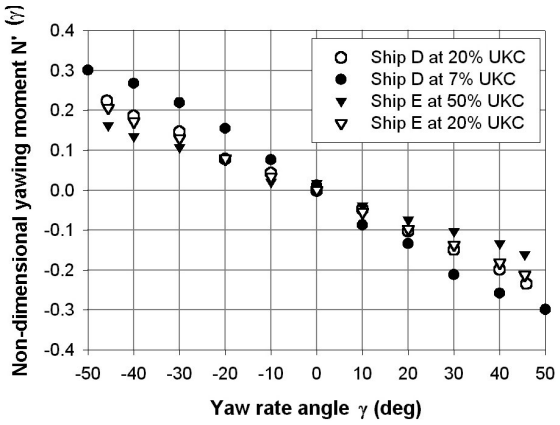

Fig. 17 Non-dimensional yawing moment $N'^{(\gamma)}$ as function of yaw rate angle.

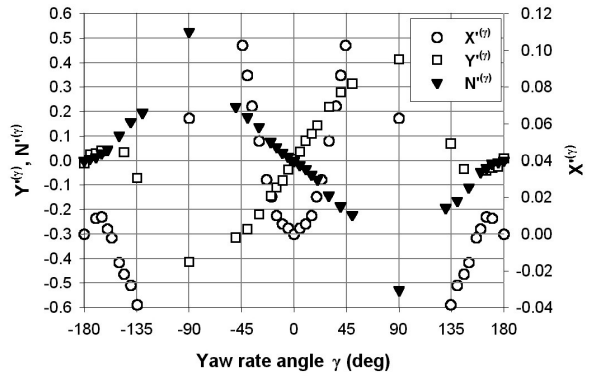

Fig. 18 Four quadrants tabular models for forces and yawing moment (E at 20% UKC).

For the ship moving astern the scatter on the non-dimensional longitudinal force $X'^{(\gamma)}$ is important.

5.3 Combination of sway and yaw: additional forces

Cross flow effects are partly included in the lateral forces and yawing moments due to pure swaying and pure yawing. Additional forces and moment measured during harmonic yaw tests with constant drift angle are subject to errors as the values are small. In figure 19 the following force is shown for the tanker at 50% UKC as a function of $\mathrm{Arc\,tan}(rl/v)$:

$$Y'^{(\beta)}(u,v,0)+Y'^{(\beta,\gamma)}(0,v,r) = \frac{Y_{Total}-(Y_f-mx_G)\dot{r}-\left(Y^{(\gamma)}(u,0,r)-mur\right)}{\frac{1}{2}\rho L_{PP}d\left(v^2+(rl)^2\right)} \quad (15)$$

with Y_{Total} the measured total hull force.

A comparable figure as figure 19 can be drawn up for the yawing moment.

The scatter occurring at angles $\mathrm{Arc\,tan}(rl/v)$ around 0° and 180° can be reduced by executing tests at higher drift angles ($\beta \geq 5°$), possibly together with a small yaw amplitude and a moderate test frequency.

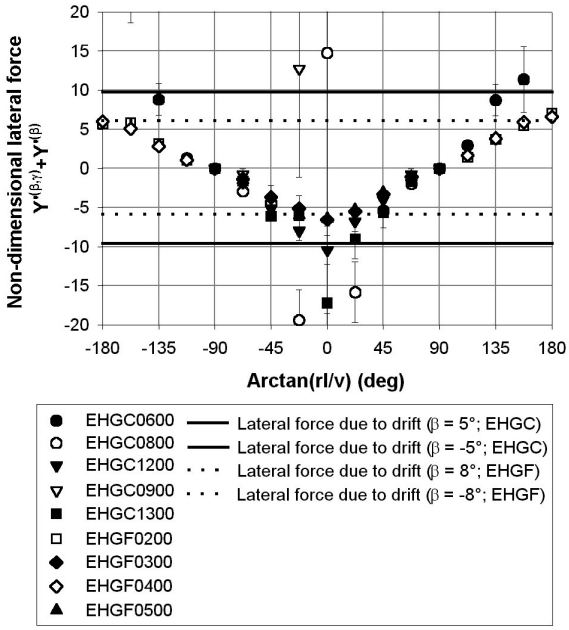

Fig. 19 Non-dimensional lateral force as a sum of an additional force due to a combination of yawing and drifting and the force due to pure drifting (E at 50% UKC, see table 5 for test parameters).

Table 5 Test parameters for tanker at 50% UKC

Run	F_n	β	ψ_A	ω'
EHGC06	0.065	2.5°	15°	2.2
EHGC08	0.065	-2.5°	15°	2.2
EHGC12	0.065	-5.0°	15°	2.2
EHGC09	0.065	-2.5°	25°	2.2
EHGC13	0.065	-5.0°	25°	2.2
EHGF02	0.065	8.0°	10°	2.9
EHGF03	0.065	-8.0°	10°	2.9
EHGF04	0.065	8.0°	20°	1.4
EHGF05	0.065	-8.0°	20°	1.4

The relationship between the cross-coupling force and moment and the angle $\mathrm{Arc\,tan}(rl/v)$ is displayed in figure 20 for the tanker at an under keel clearance of 20%.

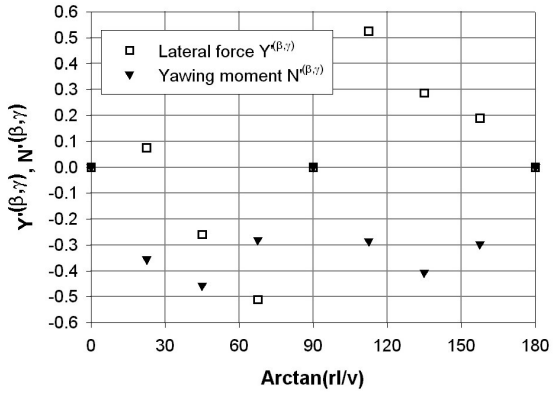

Fig. 20 Additional lateral force and yawing moment due to a combination of sway and yaw (tanker E at 20% UKC).

6. CONCLUSIONS AND PRELIMINARY GUIDELINES

The test results discussed in this paper belong to an extensive research program on mathematical modelling of ship manoeuvring in shallow water conditions based on captive model testing.

The introduction of full guidelines for physical model testing in shallow water, however, requires a further step in this research:

- the development of mathematical models describing the influence of propeller and rudder action
- the validation of the mathematical models obtained from captive model test results, based on full scale trials.

Nevertheless, preliminary guidelines can be formulated:

- The horizontal forces and yawing moment measured during captive model tests in shallow and very shallow water conditions ($h/d \leq 1.5$) are clearly influenced by the selected test parameters. In deep water conditions, this influence is negligible.
- The choice of the parameters determining the harmonic captive tests highly affects the most important acceleration derivatives, the added mass due to sway and the added moment of inertia due to yaw. The added mass due to sway is subject to non-stationary effects both for slender and full ships. The execution of alternative sway tests does not solve the problem. For the added moment of inertia, especially the results for slender ships are influenced by the test parameters.
- At equal water depth to draft ratio, the non-dimensional velocity dependent lateral force due to pure drift and the non-dimensional velocity dependent yawing moment due to pure yaw, respectively, are almost equal for the tanker and the container carrier.
- Yaw amplitude and frequency are test parameters with important influence on the velocity dependent lateral force due to pure yaw. This influence is partly, but not completely, caused by an increasing sinkage occurring at maximum yaw velocity during harmonic yaw tests.
- In order to obtain tabular hull models for four quadrants of operation, oscillating sway or yaw tests with zero forward velocity are required to determine the cross flow effects at 90° drift angle or yaw rate angle. Measured values are restricted to the first oscillation cycle as memory effects are generated due to the motion of the ship model through its own wake.

Harbour manoeuvres assisted by tugs can be very diverse, so that mathematical manoeuvring models covering four quadrants of operation and simulating the hydrodynamic hull forces and moments in a realistic way are required. The development of generally accepted guidelines for physical model testing techniques in shallow and very shallow water conditions is recommended, as numerical methods based on CFD calculations are still not satisfactory.

REFERENCES

[1] Kose K., Misiag W.A., Inoue K. “Can one have a general, standardized maneuvering model?”, IMSF Workshop, Florida, 1995

[2] Ohmori, T. “A study on hydrodynamic characteristics of a maneuvering ship in shallow water by a finite-volume method”, International Symposium and Workshop on Forces Acting on a Maneuvering Vessel, France, pp. 1-6B, 1998

[3] Oltmann P., Sharma S.D. “Simulation of combined engine and rudder maneuvers using an improved model of hull-propeller-rudder interactions”, Fifteenth Symposium on Naval Hydrodynamics, pp. 83-108, 1985

[4] Crane C.L. “Maneuvering trials of a 278 000-DWT Tanker in Shallow and Deep Waters”, Transactions of the SNAME, Vol. 87, pp. 251-283, 1979

[5] Martinussen K., Ringen E. “Manoeuvring prediction during design stage”, International Workshop on Ship Manoeuvrability at the Hamburg Ship Model Basin, pp. 1-21, 2000

[6] Eloot K., Vantorre M. “Non-conventional captive manoeuvring tests”, International Workshop on Ship Manoeuvrability at the Hamburg Ship Model Basin, Paper No. 3 20 pp., 2000

[7] The Research Committee of Dynamic Performance, Manoeuvring and Control Section “Prediction of manoeuvrability of a ship”, Bulletin of the Society of Naval Architects of Japan No. 668, 1985

[8] Eloot K., Vantorre M. “Alternative captive model tests, possibilities and limitations”, International Symposium and Workshop on Forces Acting on a Maneuvering Vessel, France, pp. 1-10J, 1998